Cancer Letters 444 (2019) 162–174

Contents lists available at ScienceDirect

Cancer Letters

journal homepage: www.elsevier.com/locate/canlet

Original Articles

S897 phosphorylation of EphA2 is indispensable for EphA2-dependent nasopharyngeal carcinoma cell invasion, metastasis and stem properties

Jiao-Yang Li[a,b], Ta Xiao[a,c], Hong-Mei Yi[a,b], Hong Yi[a,b], Juan Feng[a,b], Jin-Feng Zhu[a,b], Wei Huang[a,b], Shan-Shan Lu[a,b], Yan-Hong Zhou[d], Xin-Hui Li[a,b], Zhi-Qiang Xiao[a,b,*]

[a] *Research Center of Carcinogenesis and Targeted Therapy, Xiangya Hospital, Central South University, Changsha, Hunan, 410008, China*
[b] *The Higher Educational Key Laboratory for Cancer Proteomics and Translational Medicine of Hunan Province, Xiangya Hospital, Central South University, Changsha, Hunan, 410008, China*
[c] *Institute of Dermatology, Chinese Academy of Medical Sciences and Peking Union Medical College, Nanjing, Jiangsu, 210042, China*
[d] *Cancer Research Institute, Xiangya Medical School, Central South University, Changsha, Hunan, 410078, China*

ARTICLE INFO

Keywords:
PS897-EphA2
Nasopharyngeal carcinoma
Metastasis
Cancer stemness
Signaling pathway

ABSTRACT

Our phosphoproteomics identified that phosphorylation of EphA2 at serine 897 (pS897-EphA2) was significantly upregulated in the high metastatic nasopharyngeal carcinoma (NPC) cells relative to non-metastatic NPC cells. However, the role and underlying mechanism of pS897-EphA2 in cancer metastasis and stem properties maintenance remain poorly understood. In this study, we established NPC cell lines with stable expression of exogenous EphA2 and EphA2-S897A using endogenous EphA2 knockdown cells, and observed that pS897-EphA2 maintained EphA2-dependent NPC cell *in vitro* migration and invasion, *in vivo* metastasis and cancer stem properties. Using phospho-kinase antibody array to identify signaling downstream of pS897-EphA2, we found that AKT/Stat3 signaling mediated pS897-EphA2-promoting NPC cell invasion, metastasis and stem properties, and Sox-2 and c-Myc were the effectors of pS897-EphA2. Immunohistochemistry showed that pS897-EphA2 was positively correlated with NPC metastasis and negatively correlated with patient overall survival. Moreover, ERK/RSK signaling controlled serum-induced pS897-EphA2 in NPC cells. Collectively, our results demonstrate that pS897-EphA2 is indispensable for EphA2-dependent NPC cell invasion, metastasis and stem properties by activating AKT/Stat3/Sox-2 and c-Myc signaling pathway, suggesting that pS897-EphA2 can serve as a therapeutic target in NPC and perhaps in other cancers.

1. Introduction

Nasopharyngeal carcinoma (NPC) is a head and neck cancer that shows a distinct endemic distribution with a high prevalence in Southern China and Southeast Asia, where the annual incidence rate is approximately 25-fold higher than that in the Western world [1]. NPC is a highly malignant cancer which often invades adjacent regions and metastasizes to regional lymphnodes and distant organs at the time of diagnosis [2]. Radiotherapy is the major therapeutic modality used to treat NPC, and most NPC patients can be cured if the disease is diagnosed and treated at an early stage. However, 20%–30% of patients will develop recurrence and metastasis after therapy [3]. Therefore metastasis is a major cause of treatment failure in many NPC patients.

Eph receptors belong to a large family of receptor tyrosine kinases (RTKs), and are key regulators of both normal development and disease [4,5]. Perturbation of Eph receptor and ligand system has been observed in the various types of human cancers [6]. Particularly, EphA2 is the most frequently affected Eph receptor in human cancers. EphA2 is often overexpressed and accompanied by the loss of its ligand Ephrin-A1 in human cancers, where it promotes invasion and metastasis [5,7], induces epithelial-mesenchymal transition (EMT) [8], and maintains cancer stem properties [9,10] through a ligand-independent mechanism. In contrast, EphA2 inhibits cancer cell migration and invasion upon Ephrin-A1 stimulation through a ligand-dependent mechanism [6,7].

Previous studies indicate that the phosphorylation of EphA2 at serine 897 (pS897-EphA2) plays a key role in the ligand-independent functions of EphA2 [7,11–14]. The ligand-independent promotion of cancer cell migration and invasion by EphA2 requires pS897-EphA2, which is induced by AKT or RSK (ribosomal S6 kinase) [7,14]. Although EphA2 has been shown to maintain cancer stem properties through a ligand-independent mechanism [9,10], the roles of pS897-EphA2 in

---

[*] Corresponding author. Research Center of Carcinogenesis and Targeted Therapy, Xiangya Hospital, Central South University, Changsha, Hunan, 410008, China.
E-mail address: zqxiao2001@hotmail.com (Z.-Q. Xiao).

https://doi.org/10.1016/j.canlet.2018.12.011
Received 29 September 2018; Received in revised form 4 December 2018; Accepted 11 December 2018

cancer stem properties maintenance are poorly understood [13], and the signals downstream of pS897-EphA2 underlying its metastasis promotion and cancer stem properties maintenance need to be elucidated. We recently used phosphoproteomics to search proteins relative to NPC metastasis, and found that pS897-EphA2 was significantly upregulated in the high metastatic NPC cells relative to non-metastatic NPC cells, suggesting that pS897-EphA2 plays a crucial role in the NPC metastasis.

In the present study, we try to determine whether and how pS897-EphA2 promotes NPC cell invasion and metastasis and maintains cancer stem properties. Our results demonstrate that pS897-EphA2 is indispensable for EphA2-dependent NPC cell invasion, metastasis and stem properties, and AKT/Stat3/Sox-2 and c-Myc signaling pathway mediates the phenotypes of pS897-EphA2, suggesting that pS897-EphA2 can serve as an attractive therapeutic target in NPC and perhaps in other cancers.

2. Materials and methods

2.1. Patients and tissue specimens

The one hundred and twenty-seven formalin-fixed and paraffin-embedded archival NPC tissue specimens, twenty lymphonode metastases paired with primary NPCs and thirty normal nasopharyngeal mucosa between Jan 2007 and Dec 2009 were obtained from the First Hospital of Chenzhou City (China) at the time of diagnosis before any therapy. In addition, eight fresh NPC biopsies were also collected. On the basis of the 1978 WHO classification [15], all tumors were histopathologically diagnosed as poorly differentiated squamous cell carcinomas (WHO type III). The clinical stage of the patients was classified and reclassified according to the AJCC criteria as described in the seventh edition of the AJCC cancer staging manual. All the patients underwent radiochemotherapy and were given follow-up. The follow-up period at the time of analysis was 9–83 months (average, 48 ± 16.5). The total survival was defined as the time from diagnosis to the date of cancer-related death or when censured at the latest date if patients were still alive. The clinicopathological features of the patients used in the present study are shown in Supplemental Table 1.

2.2. Plasmids

Plasmid expressing EphA2 or EphA2-S897A cDNA and control plasmid pBabepuro were a gift from Dr. B Wang (Case Western Reserve University, Cleveland, USA) [7]. Lentiviral GV101 vector expressing EphA2 shRNA or scramble non-target shRNA were established by Genechem (Shanghai, China), and confirmed by sequencing. The target for human EphA2 shRNA is 5′-CAGCCTTCGGACAGACATA-3′ that is located in the 3‘UTR of EphA2 mRNA. The knockdown efficiency of the EphA2 shRNA has been validated [16].

2.3. Cell lines and culture

High metastatic 5–8F and non-metastatic 6–10B NPC cell lines were established and kindly gifted by Dr. HM Wang of the Cancer Center, Sun Yat-sen University, China [17,18]. Poorly differentiated CNE2 and highly differentiated CNE1 NPC cell lines have been described previously by us [19,20]. Cells were cultured in RPMI-1640 medium supplemented with 10% fetal bovine serum (Life Technologies) at 37 °C in 5% CO_2. The cell lines were authenticated by short tandem repeat profiling prior to use, and were routinely tested negative for mycoplasma contamination using 4,6-diamidino-2-phenylindole staining.

2.4. Quantitative PM phosphoproteome analysis using $^{16}O/^{18}O$ labeling and LC-MS/MS

Differential plasma membrane (PM) proteome analysis in 5–8F and 6–10B NPC cells was performed as described previously by us (Supplemental Fig. 1A) [21–23]. MS data processing and database search for protein identification and relative quantification were performed as described by Chi LM et al. [24]. An on-line PhosphoSitePlus™ system biology resource (http://www.phosphosite.org/) was used to annotate the phosphorylation modification sites of identified proteins.

2.5. Establishment of NPC cell lines expressing exogenous EphA2 or EphA2-S897A using endogenous EphA2 knockdown cells

Lentiviral GV101 vector expressing EphA2 shRNA or scramble shRNA infected high metastatic 5–8F and poorly differentiated CNE2 NPC cell lines respectively, cells were selected using neomycin for two weeks, and 5–8F and CNE2 cell lines with stable endogenous EphA2 knockdown and control cell lines were obtained. Plasmid expressing EphA2 or EphA2-S897A cDNA and control plasmid pBabepuro were transfected into 5–8F and CNE2 NPC cell lines with endogenous EphA2 knockdown using Lipofectamine 2000 (Life Technologies) respectively. Cells were selected using puromycin for two weeks, and 5–8F and CNE2 cell lines with the stable expression of exogenous EphA2 or EphA2-S897A and control cell lines were obtained.

2.6. Identification of differential phospho-kinases by human phospho-kinase antibody array

Membranes (#ARY003B, R&D) already captured with antibodies were blocked with blocking buffer at room temperature for 1 h. Cell lysates extracted from 5 - 8F cells with the stable expression of exogenous EphA2-S897A and EphA2 (1 mg per sample) were incubated with the membranes at 4 °C overnight, followed by three washes in washing buffer. Biotinylated antibody cocktail, streptavidin conjugated to horseradish-peroxidase and chemiluminescent detection reagents were subsequently added, and chemiluminescence was detected in the same manner as a Western blot analysis.

2.7. Cell migration and invasion assay

Cell migration and Matrigel invasion assays were performed as described previously by us [18].

2.8. Sorting of side population cells by flow cytometry

Sorting of side population cells was performed by flow cytometry as described previously by us [25]. The detailed procedures are described in Supplementary information.

2.9. QRT-PCR

Real-time qRT-PCR was performed to detect the expression of Sox-2, c-Myc and ALDH1A1 in the NPC cells as described previously by us [18]. The primers used for the amplification of the indicated genes are listed in Supplemental Table 2.

2.10. Western blot

Western blot was performed to detect the expression of proteins in the indicated NPC cells and tissues as described previously by us [18,19].

2.11. Dual luciferase reporter assay

Dual luciferase reporter assay was performed to detect the transcriptional activity of human Stat3 in the indicated NPC cells as described previously by us [18]. The detailed procedures are described in Supplementary information.

2.12. Tumor formation and experimental lung metastasis

Nude female mice (BALB/c nu/nu) and non-obese diabetic/severe combined immunodeficient (NOD/SCID) mice that were four weeks old were obtained from the Laboratory Animal Center of Central South University (Changsha, China), and were maintained under specific pathogen-free conditions. For tumor formation experiment, serial dilutions of the NPC cells were subcutaneously injected into NOD-SCID mice (n = 8 mice each). The mice were monitored daily for palpable tumor formation. Tumor volume (in cm^3) was measured by caliper measurements and calculated by using the modified ellipse formula (volume = length × $width^2/2$). For experimental lung metastatic experiment, mice (n = 10 mice each) were injected intravenously with 1×10^6 NPC cells/mouse via the tail vein. At the end of the five weeks, mice were sacrificed by cervical dislocation, and subcutaneous xenografts and lungs were removed. Lung surface metastases were examined macroscopically. The tissues were embedded in paraffin for H.E. and immunohistochemical staining.

2.13. Immunohistochemistry and immunofluorescence

Immunohistochemistry on the paraffin-embedded tissue sections and immunofluorescent staining of the indicated cells were performed as described previously by us [18,19]. The detailed procedures are described in Supplementary information.

2.14. Statistical analysis

All experiments were carried out at least 3 times. Data were presented as the mean ± standard deviation. Statistical analysis was conducted using SPSS 22.0 statistical software package. For comparisons between two groups, a Student's *t*-test was used, and for analysis with multiple comparisons, One-way ANOVA, followed by Turkey's post-hoc analysis was used. Survival curves were obtained by using Kaplan–Meier method, and comparisons were made by using log-rank test. Univariate and multivariate survival analyses were conducted on all parameters by using Cox proportional hazards regression model. The Spearman rank correlation coefficient was used to determine the correlation between the expression levels of two proteins in the NPC tissues based on IHC results. All statistical tests were 2-sided. *P* values less than 0.05 were considered to be statistically significant.

2.15. Ethics statement

This study was approved by the Medical Ethics Committee of Xiangya Hospital, Central South University, China. All animal experiments were undertaken in accordance with the Guide for the Care and Use of Laboratory Animals of Central South University, with the approval of the Scientific Investigation Board of Central South University. As only archived tumor specimens were included in this study, the ethics committee waived the need for consent and patient records/information were analyzed anonymously.

3. Results

3.1. Identification of pS897-EphA2 as a protein associated with NPC metastasis and poor patient prognosis

Quantitative PM phosphoproteome analysis was performed to screen the differential phospho-proteins in the high metastatic 5–8F and non-metastatic 6–10B NPC cells. As a result, a total of thirteen differential phospho-proteins were identified (Supplemental Table 3). Among them, pS897-EphA2 was significantly upregulated in the 5–8F cells relative to 6–10B cells (Supplemental Fig. 1B and Supplemental Table 3), which was confirmed by Western blot (Fig. 1A). We further detected the levels of pS897-EphA2 in the eight fresh NPC biopsies by Western blot, and observed that it was significantly increased in the NPCs with metastasis relative to NPCs without metastasis (Fig. 1A). Next, we analyzed the levels of pS897-EphA2 and Ephrin-A1 in 127 NPCs with the different metastatic potentials, 20 paired neck lymphonode metastases (LNMs) and 30 normal nasopharyngeal mucosa (NNM) by immunohistochemistry (IHC). The results showed that pS897-EphA2 was significantly increased in the LNMs relative to paired NPCs, in the NPCs with metastasis relative to NPCs without metastasis, and not detectable in the most of NNM (Fig. 1B and Supplemental Table 4); pS897-EphA2 was significantly correlated with lymphonode and distant metastasis (Supplemental Table 5), and markedly reduced patient overall survival (Fig. 1C). A univariate and multivariate Cox regression analysis showed that pS897-EphA2 was an independent predictor for patient overall survival (Supplemental Table 6). These results indicate that pS897-EphA2 is associated with NPC metastasis and can serve as a predictor for NPC patient prognosis.

Our IHC showed that Ephrin-A1 expression was significantly reduced in the NPCs relative to paired NNM, in the NPCs with metastasis relative to NPCs without metastasis, and was not detectable in the most of LNMs (Fig. 1B and Supplemental Table 4), *i.e.* the loss of Ephrin-A1 expression during NPC progression, indicating that the NPC promotion of pS897-EphA2 is ligand-independent [7,11–14]. Moreover, we observed that exogenous Ephrin-A1 stimulation caused the obvious downregulation of pS897-EphA2 and EphA2 (Supplemental Fig. 2A), and inhibited cell migration and invasion, side-population cells fraction and tumorsphere formation in the 5–8F and CNE2 cell lines with high EphA2 expression (Supplemental Fig. 2B ~ D), supporting that the NPC promotion of pS897-EphA2 is ligand-independent.

3.2. PS897-EphA2 maintains EphA2-dependent NPC cell migration, invasion and metastasis

We first established 5–8F and CNE2 NPC cell lines with stable knockdown of endogenous EphA2 by shRNA targeting to EphA2 mRNA 3‘UTR because both cell lines had high endogenous EphA2 expression (Supplemental Figs. 3A and B). The results showed that knockdown of EphA2, concomitant with the loss of pS897-EphA2 (Supplemental Fig. 3B), led to an obvious reduction in ligand-independent cell migration, invasion, and tumorsphere formation (Supplemental Figs. 3C and D). To explore the biological functions of pS897-EphA2, we transfected plasmid expressing shRNA-resistant cDNA encoding EphA2 or EphA2-S897A into the two cell lines with endogenous EphA2 knockdown respectively, and established 5–8F and CNE2 cell lines with stable expression of exogenous EphA2 (EphA2-WT) or EphA2-S897A (EphA2-SA) (Fig. 2A). Western blot analysis revealed that the established 5–8F or CNE2 cell lines expressed the equivalent levels of exogenous EphA2-WT and EphA2-SA, and S897A mutation abolished pS897-EphA2, but didn't affect the tyrosine phosphorylation of EphA2 at Y588 (pY588-EphA2) (Fig. 2A). Next, we analyzed the effects of EphA2-WT and EphA2-SA on the metastatic potentials of NPC cells, and observed that EphA2-WT dramatically increased NPC cell migration and invasion *in vitro,* whereas EphA2-SA failed to do it as compared to endogenous EphA2 knockdown (Fig. 2B), indicating that S897A mutation abolished the effects of EphA2-WT on NPC cell migration and invasion *in vitro*. Moreover, we tested the effects of EphA2-WT and EphA2-SA on NPC cell metastasis. As shown in Fig. 2C and D, EphA2-WT markedly increased the lung metastases of NPC cells, whereas EphA2-SA failed to do it as compared to endogenous EphA2 knockdown, indicating that S897A mutation abolished the effects of EphA2-WT on NPC cell metastasis *in vivo*. Together, these results demonstrate that pS897-EphA2 maintains EphA2-dependent NPC cell migration, invasion and metastasis.

3.3. PS897-EphA2 maintains EphA2-dependent NPC cell stem properties

Side-population (SP) cells, a small population of cells from cancer

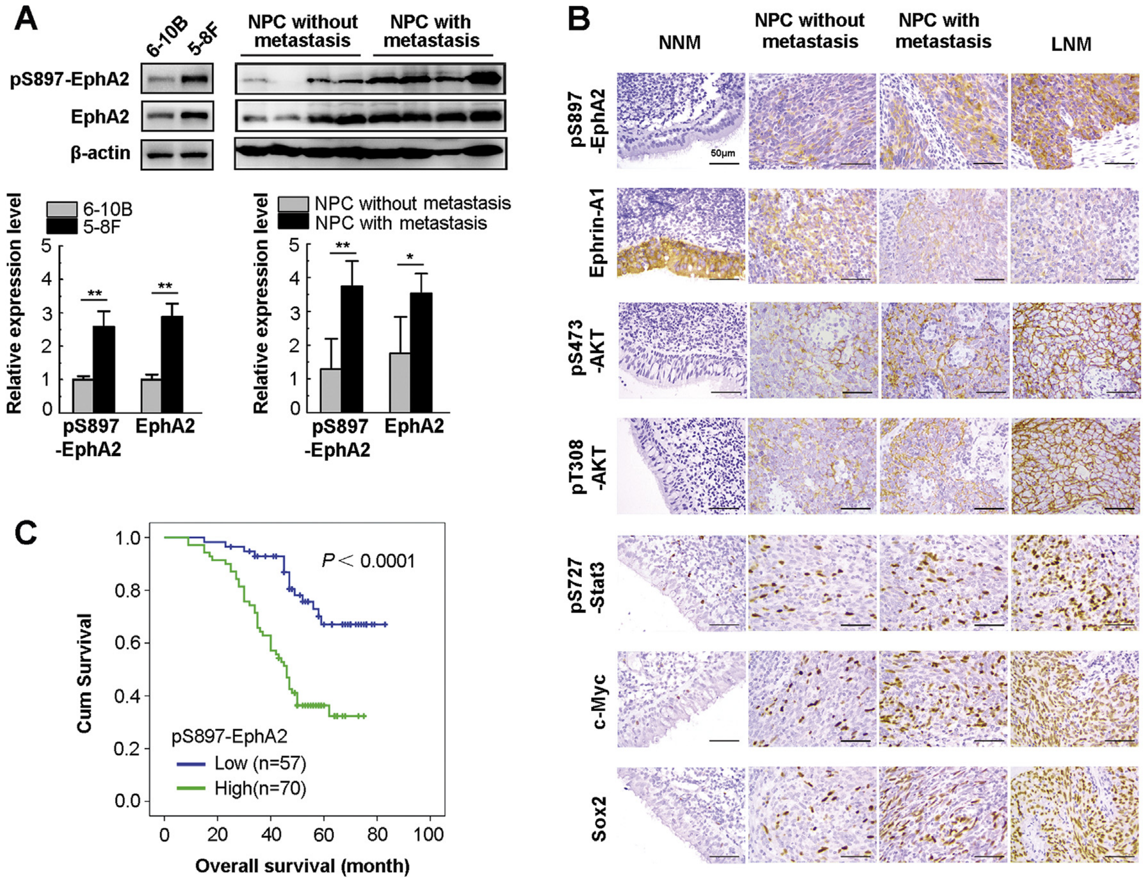

Fig. 1. PS897-EphA2 is correlated with NPC metastasis and poor patient prognosis. (**A**) Western blot analysis showing the expression levels of pS897-EphA2 and EphA2 in the 5–8F and 6–10B cells (*left*), as well as in the eight fresh NPC tissues (*right*). Numbers represent mean ± SD. $^{*}P < 0.05$; $^{**}P < 0.01$. (**B**) Immunohistochemistry showing the expression levels of pS897-EphA2, Ephrin-A1, p-AKT, p-Stat3, c-Myc and Sox-2 in the normal nasopharyngeal mucosa (NNM), NPC without metastasis, NPC with metastasis and paired lymphonode metastasis (LNM). Scale bars = 50 μm. (**C**) Kaplan-Meier survival analysis for 127 NPC patients according to the levels of pS897-EphA2. Log-rank test was used to calculate *P* value.

cell lines, can efflux lipophilic fluorescent dyes and are enriched in cancer stem cells [26,27]. Accordingly, we analyzed the effect of EphA2-WT and EphA2-SA on the NPC SP cell fraction. As shown in Fig. 3A, EphA2-WT significantly increased SP cell fraction, whereas EphA2-SA had not obvious effect on it as compared to endogenous EphA2 knockdown, indicating that S897A mutation abolished the effect of EphA2-WT on NPC SP cell fraction. Tumorsphere formation is an *in vitro* sensitive assay for determining the self-renewal capacity of cancer stem cells (CSCs) *in vitro* and the abundance of CSCs in malignant populations [28,29]. Therefore, we analyzed the effect of EphA2-WT and EphA2-SA on the tumorsphere formation of NPC cells. The result showed that EphA2-WT significantly enhanced tumorsphere formation, which was observed over two further serial passages, whereas EphA2-SA failed to do it as compared to endogenous EphA2 knockdown (Fig. 3B), indicating that S897A mutation abolished the effect of EphA2-WT on the tumorsphere formation of NPC cells. Next, we analyzed the effect of EphA2-WT and EphA2-SA on the expression of several known NPC stem markers including c-Myc, Sox-2 and ALDH1A1 [30–33]. As shown in Fig. 3C, EphA2 substantially increased the mRNA and protein expression of the three stem markers in the NPC cells, whereas EphA2-SA had not obvious affection on their expression as compared to endogenous EphA2 knockdown, indicating that S897A mutation abolished the effect of EphA2-WT on the stem marker expression of NPC cells.

Increasing evidences have highlighted a link between EMT and CSCs [34]. It has been reported that EMT generates cells with the stem properties [35]. Therefore, we analyzed the effect of EphA2-WT and EphA2-SA on the expression of representative EMT markers in NPC cells. We observed that EphA2-WT significantly upregulated Vimentin and N-cadherin while significantly downregulated E-cadherin, *i.e.* that EphA2-WT induced EMT-like alterations, whereas EphA2-SA only had slight affection on the expression of the three EMT markers as compared to endogenous EphA2 knockdown (Fig. 3D), suggesting that S897A mutation abolished the effect of EphA2-WT on the EMT-like alterations of NPC cells. Collectively, our results demonstrate that pS897-EphA2 maintains EphA2-dependent NPC cell stem properties.

3.4. PS897-EphA2 maintains EphA2-dependent tumor initiating capacity of NPC cells in vivo

To test whether p-EphA2-S897 affects tumor-initiating capacity of NPC cells *in vivo*, serial dilutions of 5–8F and CNE2 NPC cells expressing exogenous EphA2-WT or EphA2-SA (1×10^2, 1×10^3, 1×10^4, 1×10^5) and their control cells with endogenous EphA2 knockdown were subcutaneously injected into NOD-SCID mice. After implantation, tumor development and growth were monitored for five weeks. The results showed that EphA2-WT markedly increased the tumor incidence and growth rate when 1×10^3, 1×10^4 or 1×10^5 cells were injected, whereas EphA2-SA failed to do it as compared to endogenous EphA2 knockdown (Fig. 4), indicating that S897A mutation abolished the effects of EphA2-WT on *in vivo* tumor-initiating capacity of NPC cells. When 1×10^2 cells were injected, both the experimental and vector control cells did not form tumors at week 5. The results indicate that pS897-EphA2 maintains EphA2-dependent tumor initiating capacity of NPC cells *in vivo*.

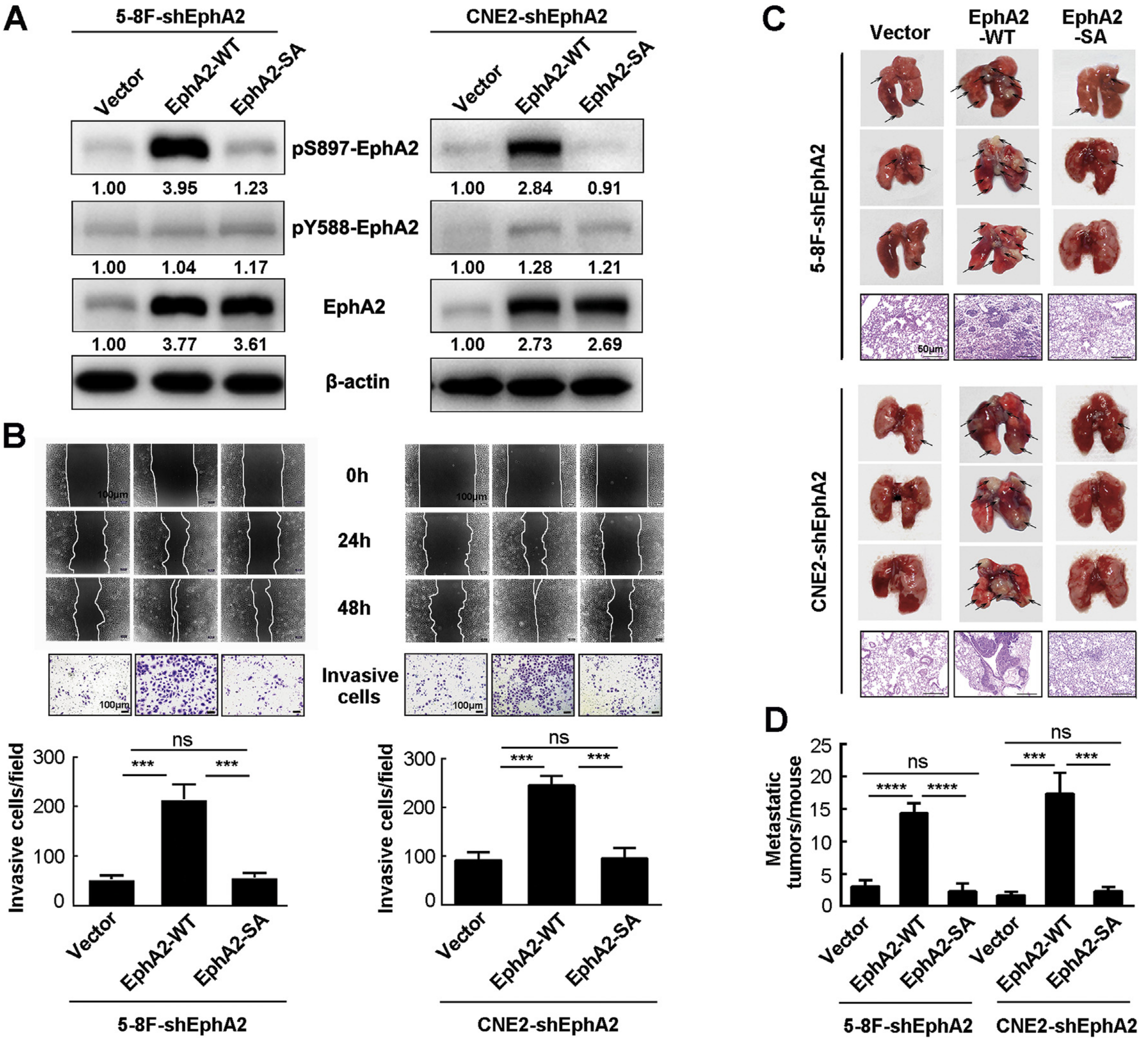

Fig. 2. PS897-EphA2 maintains EphA2-dependent NPC cell migration, invasion and metastasis (**A**) Establishment of 5–8F and CNE2 cell lines with the stable expression of exogenous EphA2 (EphA2-WT) or EphA2-S897A (EphA2-SA) using endogenous EphA2 knockdown (shEphA2) cells and their control cell lines with endogenous EphA2 knockdown. (**B**) Scratch wound-healing (*top*) and Matrigel invasion assay (*middle* and *bottom*) showing the migration and invasion of NPC cells expressing EphA2-WT or EphA2-SA and their control cells. (**C**) The *in vivo* metastasis assays of NPC cells expressing EphA2-WT or EphA2-SA and control cells by using experimental lung metastasis model, $n = 10$ mice per group. The representative images of lungs and H&E staining of lung tissues showing metastatic tumors (*black arrows*). (**D**) Histogram showing the average numbers of lung surface metastases per mouse. Numbers represent mean ± SD. $^{***}P < 0.001$; $^{****}P < 0.0001$; ns, no significance.

3.5. *PS897-EphA2 activates AKT/Stat3 signaling in NPC cells*

Human phospho-kinase antibody array was used to screen the differential phospho-kinases in the 5–8F cells expressing exogenous EphA2-WT and EphA2-S897A. As shown in Fig. 5A, the levels of p-AKT (T308 and S473) and p-Stat3 (S727) were significantly decreased in the EphA2-SA-expressed 5–8F cells relative to EphA2-WT-expressed 5–8F cells, whereas p-Stat3 (Y705) level had no obvious difference in the two cell lines. Western blot analysis further showed that EphA2-WT significantly increased while EphA2-SA failed to increase the levels of p-AKT (T308 and S473) and p-Stat3 (S727) in the 5–8F and CNE2 NPC cell lines as compared to endogenous EphA2 knockdown (Fig. 5B), indicating that S897A mutation abolished the effect of EphA2-WT on the levels of p-AKT (T308 and S473) and p-Stat3 (S727). Immunofluorescent staining also showed that EphA2-WT increased while EphA2-SA failed to increase the level and membrane translocation of p-AKT (S473) (Fig. 5C). The results indicate that pS897-EphA2 activates AKT and Stat3 signaling in the NPC cells.

Previous studies have demonstrated that EphA2 recruits or interacts with the p85 regulatory subunit of PI3-kinase (PI3K) [36–38], and activates PI3K and downstream AKT [39,40]. Therefore we investigated whether pS897-EphA2 phosphorylates and activates AKT by PI3K in the NPC cells. The result showed that EphA2-WT significantly increased while EphA2-SA failed to increase p-p85 level as compared to endogenous EphA2 knockdown, indicating that S897A mutation abolished the effect of EphA2-WT on p-p85 (Fig. 5D). Moreover, PI3K inhibitor LY294002 inhibited p-AKT level in the NPC cells expressing EphA2-WT (Fig. 5D). Together, the results indicate that pS897-EphA2 activates AKT signaling through PI3K in the NPC cells.

It has been reported that there is a functional link between AKT and Stat3 signaling [41,42], in which activation of AKT induces phosphorylation of Stat3 at S727 but not Y705. Our results showed that pS897-EphA2 phosphorylated Stat3 at S727 but not Y705, whereas S897A mutation abolished the effect of EphA2-WT on p-Stat3 (Fig. 5A and B). Therefore we analyzed whether pS897-EphA2 activates Stat3 through p-AKT in the NPC cells, and observed that AKT inhibitor MK2206 decreased p-Stat3 (S727) level in the NPC cells expressing EphA2-WT, whereas transfection of plasmid expressing AKT increased p-Stat3 (S727) level in the NPC cells expressing EphA2-SA (Fig. 5E), suggesting that pS897-EphA2 activates Stat3 through AKT in the NPC

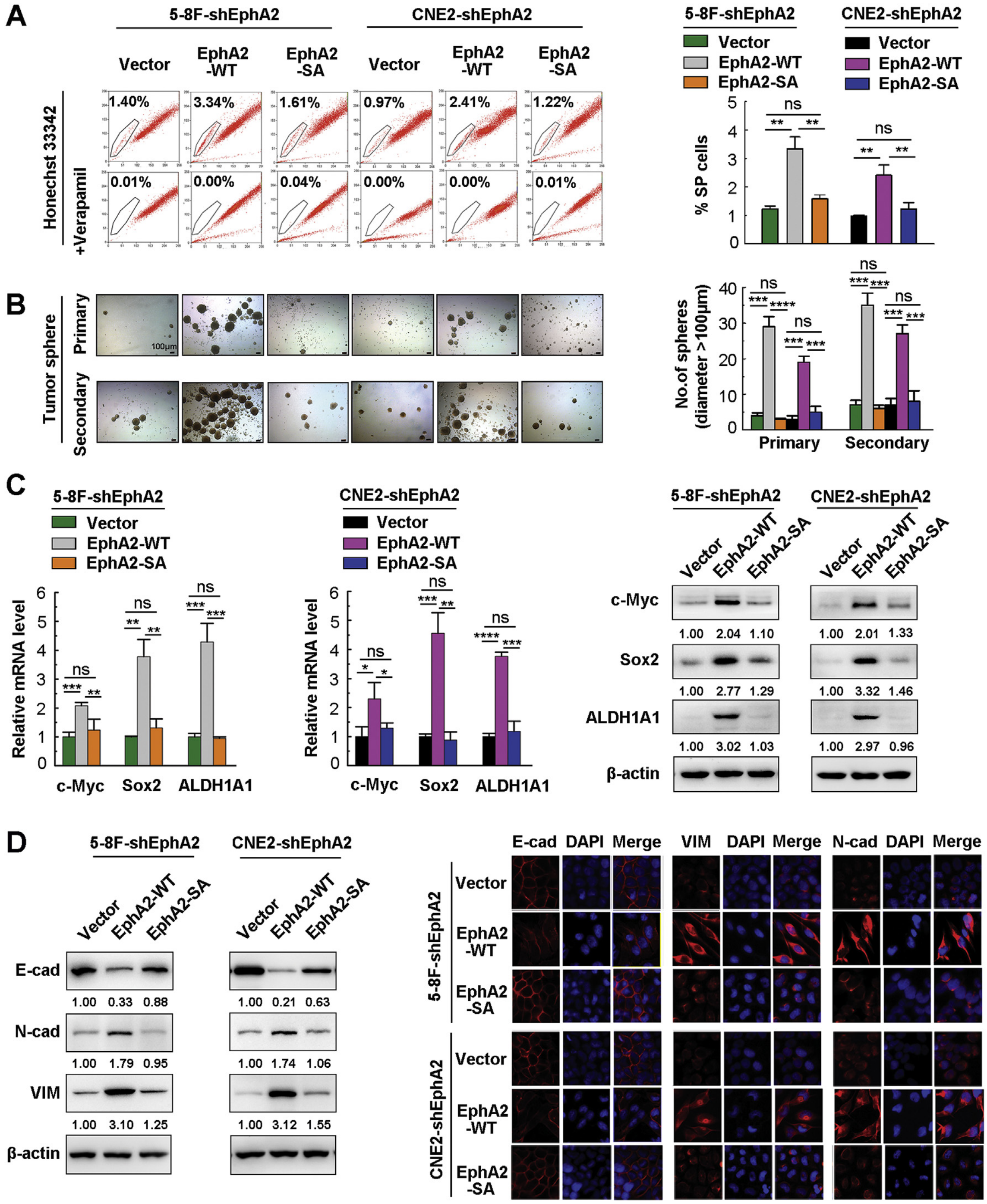

Fig. 3. PS897-EphA2 maintains EphA2-dependent NPC cell stem properties. (**A**) A representative result (*left*) and statistical analysis (*right*) of side-population (SP) cells sorted by flow cytometry in the NPC cells expressing EphA2-WT or EphA2-SA and their control cells in the absence and presence of verapamil. (**B**) A representative result (*left*) and statistical analysis (*right*) of primary and secondary tumorspheres formed by NPC cells expressing EphA2-WT or EphA2-SA and their control cells. (**C**) QRT-PCR (*left*) and Western blot analysis (*right*) showing the expression levels of c-Myc, Sox-2 and ALDH1A1 in the NPC cells expressing EphA2-WT or EphA2-SA and their control cells. (**D**) Western blot analysis (*left*) and immunofluorescent staining (*right*) showing the expression levels of E-cadherin (E-cad), N-cadherin (N-cad) and Vimentin (Vim) in the NPC cells expressing EphA2-WT or EphA2-SA and their control cells. Original magnification, × 400. Numbers represent mean ± SD. $^{*}P < 0.05$; $^{**}P < 0.01$; $^{***}P < 0.001$; $^{****}P < 0.0001$; ns, no significance.

cells.

As phosphorylation of Stat3 at S727 leads to its transcriptional activation [43], we performed a dual luciferase reporter assay to determine the effect of pS897-EphA2 on Stat3 transcriptional activity, and observed that EphA2-WT significantly increased Stat3 transcriptional activity in the NPC cells, whereas EphA2-SA failed to do it as compared to endogenous EphA2 knockdown (Fig. 5F), supporting that pS897-EphA2 activates Stat3 signaling through AKT in the NPC cells.

3.6. AKT/Stat3 signaling mediates pS897-EphA2-dependent NPC cell invasion, metastasis and stem properties

We next explore whether AKT/Stat3 signaling mediates the action of pS897-EphA2 in the NPC cells. We observed that transfection of

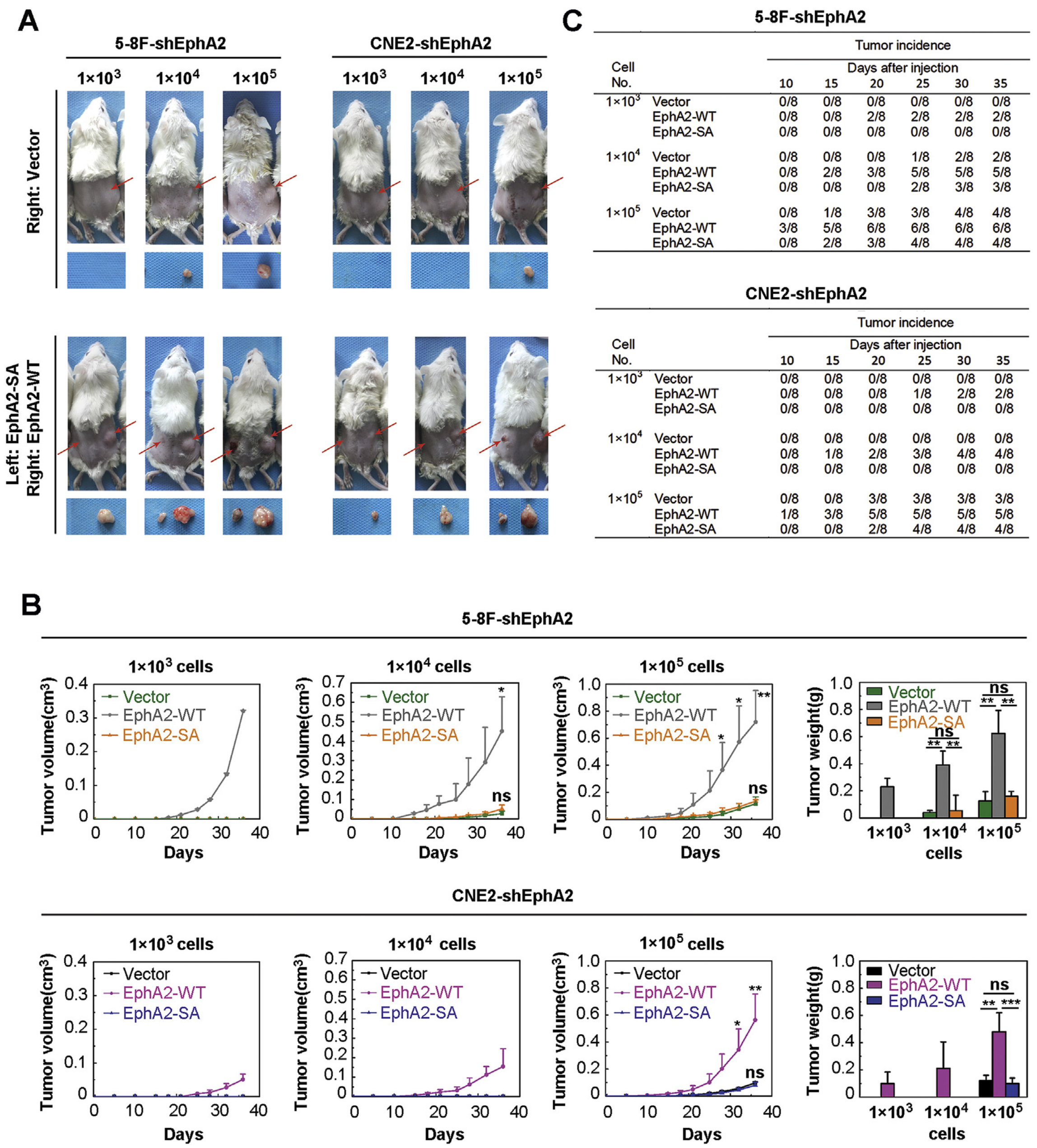

5-8F-shEphA2

Cell No.		Tumor incidence Days after injection 10	15	20	25	30	35
1×10^3	Vector	0/8	0/8	0/8	0/8	0/8	0/8
	EphA2-WT	0/8	0/8	2/8	2/8	2/8	2/8
	EphA2-SA	0/8	0/8	0/8	0/8	0/8	0/8
1×10^4	Vector	0/8	0/8	0/8	1/8	2/8	2/8
	EphA2-WT	0/8	2/8	3/8	5/8	5/8	5/8
	EphA2-SA	0/8	0/8	0/8	2/8	3/8	3/8
1×10^5	Vector	0/8	1/8	3/8	3/8	4/8	4/8
	EphA2-WT	3/8	5/8	6/8	6/8	6/8	6/8
	EphA2-SA	0/8	2/8	3/8	4/8	4/8	4/8

CNE2-shEphA2

Cell No.		Tumor incidence Days after injection 10	15	20	25	30	35
1×10^3	Vector	0/8	0/8	0/8	0/8	0/8	0/8
	EphA2-WT	0/8	0/8	0/8	1/8	2/8	2/8
	EphA2-SA	0/8	0/8	0/8	0/8	0/8	0/8
1×10^4	Vector	0/8	0/8	0/8	0/8	0/8	0/8
	EphA2-WT	0/8	1/8	2/8	3/8	4/8	4/8
	EphA2-SA	0/8	0/8	0/8	0/8	0/8	0/8
1×10^5	Vector	0/8	0/8	3/8	3/8	3/8	3/8
	EphA2-WT	1/8	3/8	5/8	5/8	5/8	5/8
	EphA2-SA	0/8	0/8	2/8	4/8	4/8	4/8

Fig. 4. PS897-EphA2 maintains EphA2-dependent tumor initiating capacity of NPC cells *in vivo*. (**A**) The representative photographs of xenograft tumors at 5 weeks after subcutaneous implantation of NPC cells expressing EphA2-WT or EphA2-SA and their control cells, $n = 8$ mice per group. (**B**) Tumor volume was periodically monitored and tumor growth curves of 1×10^3, 1×10^4 and 1×10^5 NPC cells were plotted, and average tumor weight at 5 weeks after subcutaneous implantation is also shown. (**C**) Summary data of tumor-initiation capacity of the NPC cells. Numbers represent mean ± SD. $^*P < 0.05$; $^{**}P < 0.01$; ns, no significance.

plasmid expressing AKT or Stat3 restored the expression of the three NPC stem markers, ability of cell invasion and tumorsphere formation, and SP cell fraction in the NPC cells expressing EphA2-S897A (Fig. 6A and B). IHC showed that EphA2-WT significantly increased the expression levels of p-AKT, p-Stat3, and three NPC stem markers in the lung metastases of NPC cells, whereas EphA2-SA failed to do it as compared to endogenous EphA2 knockdown (Fig. 6C). Collectively, the results demonstrate that AKT/Stat3 signaling mediates pS897-EphA2-dependent NPC invasion and metastasis and stem properties.

3.7. Sox-2 and c-Myc are the effectors of pS897-EphA2-dependent NPC cell invasion and stem properties

Our results showed that pS897-EphA2 upregulated the expression of Sox-2 and c-Myc. Because Sox-2 and c-Myc, the known direct transcriptional targets of Stat3 [44,45], play a crucial role in maintaining cancer stem properties in many malignancies including NPC [30,32,44,45], their roles in pS897-EphA2-dependent NPC invasion and stem properties were further studied. We observed that transfection of plasmid expressing Sox-2 or c-Myc restored the ability of cell invasion and tumorsphere formation and SP cell fraction in the NPC cells expressing EphA2-SA (Fig. 7). IHC showed that EphA2-WT significantly increased the expression levels of c-Myc and Sox-2 in the lung metastases of NPC cells, whereas EphA2-SA failed to do it as compared to endogenous EphA2 knockdown (Fig. 6C). These results suggest that Sox-2 and c-Myc are the effectors of pS897-EphA2-promoting NPC cell invasion and stem properties.

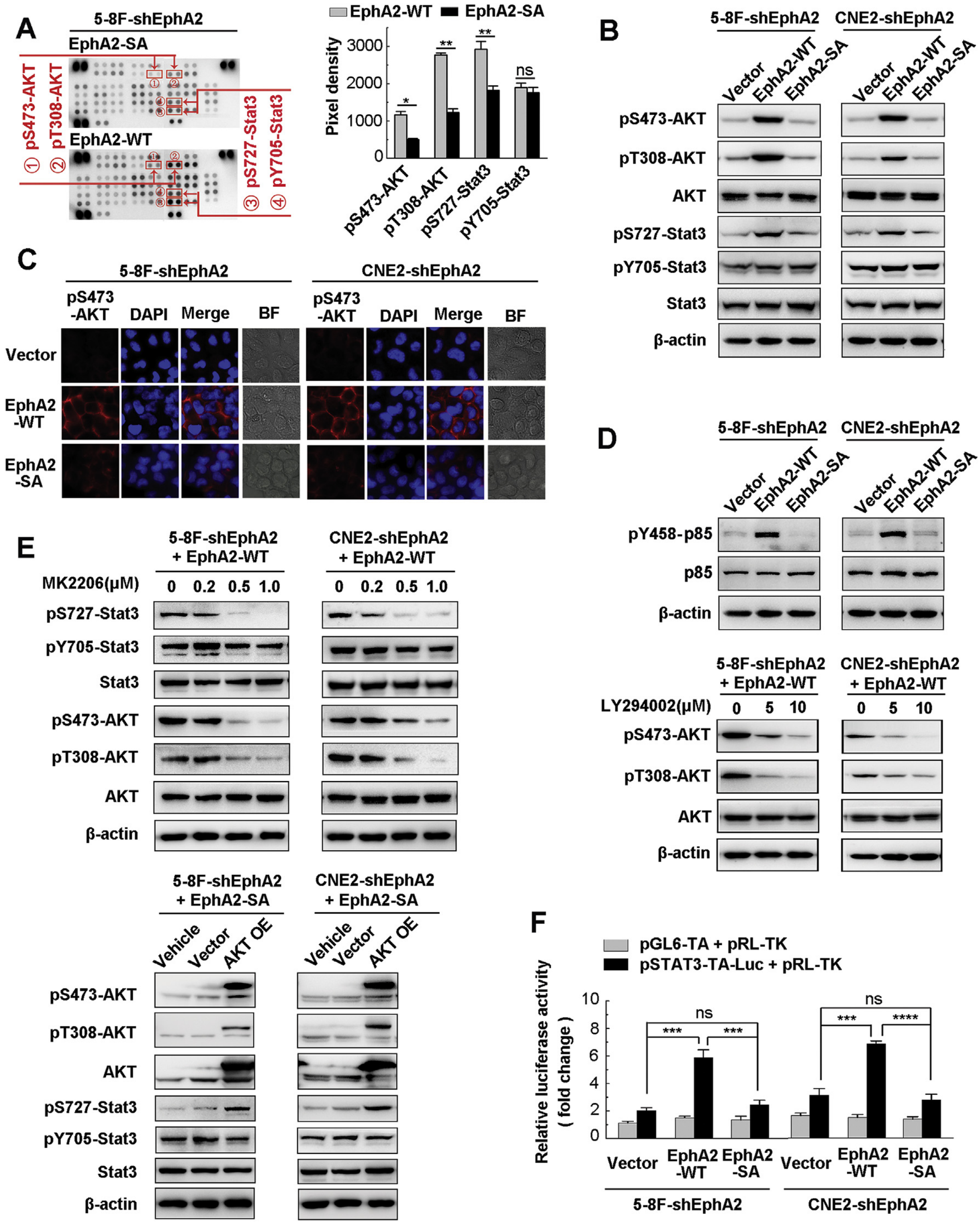

Fig. 5. PS897-EphA2 activates AKT/Stat3 signaling in NPC cells. (**A**) (*left*) A representative result of antibody array screening for the differential phospho-kinases in the 5–8F NPC cells expressing EphA2-WT and EphA2-SA. (*right*) Histogram showing the levels of p-AKT and p-Stat3. (**B**) Western blot analysis showing the levels of p-AKT and p-Stat3 in the NPC cells expressing EphA2-WT or EphA2-SA and their control cells. (**C**) Representative immunofluorescent staining the levels and membrane translocation of p-AKT in the NPC cells expressing EphA2-WT or EphA2-SA and their vector control cells. Original magnification, × 400. (**D**) (*top*) Western blot analysis showing the levels of p-p85 in the NPC cells expressing EphA2-WT or EphA2-SA and their control cells. (*bottom*) Western blot analysis showing the levels of p-AKT in the EphA2-WT-expressed NPC cells treated with LY294002. (E) (*top*) Western blot analysis showing the levels of p-Stat3 and p-AKT in the EphA2-WT-expressed NPC cells treated with MK2206. (*bottom*) Western blot analysis showing the levels of p-Stat3 and p-AKT in the EphA2-SA-expressed NPC cells transfected with AKT expression plasmid and their control cells. (**F**) Luciferase reporter assay showing Stat3 transcriptional activity in the NPC cells expressing EphA2-WT or EphA2-SA and their control cells. Numbers represent mean ± SD. $*P < 0.05$; $**P < 0.01$ $***P < 0.001$; $****P < 0.0001$; ns, no significance.

3.8. Levels of pS897-EphA2, p-AKT, p-Stat3, c-Myc and Sox-2 are correlated in human NPC biopsies

Our IHC showed that the levels of pS897-EphA2, p-AKT, p-Stat3, c-Myc and Sox-2 were significantly higher in NPCs with metastasis than those in NPCs without metastasis, and in LNMs than those in primary NPCs (Fig. 1B and Supplemental Table 4). Correlation analyses revealed that there were positive correlations among pS897-EphA2, p-AKT, p-

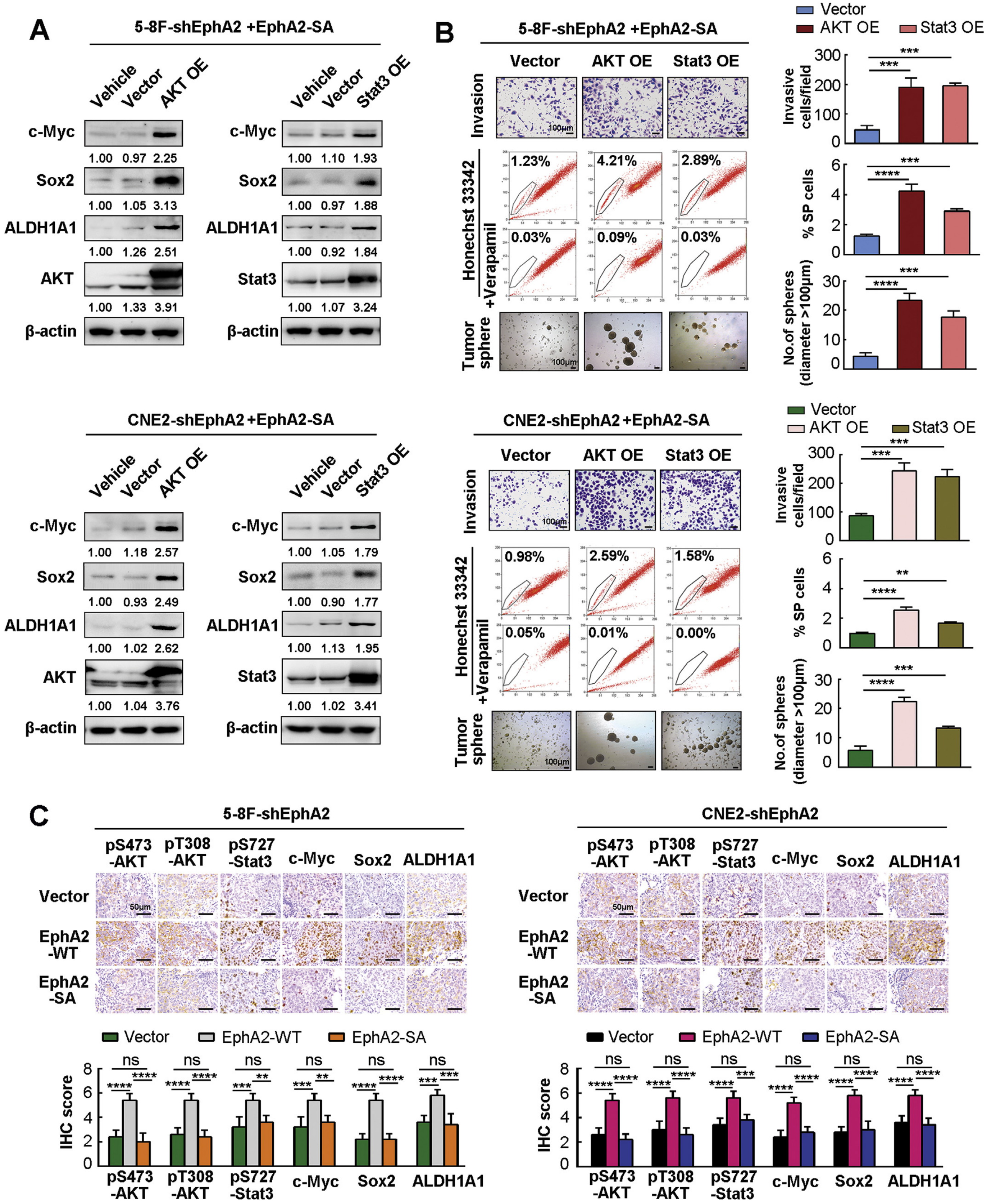

Fig. 6. AKT/Stat3 signaling mediates pS897-EphA2-dependent NPC cell invasion, metastasis and stem properties. (**A**) Western blot analysis showing the expression levels of c-Myc, Sox-2 and ALDH1A1 in the EphA2-SA-expressed NPC cells transfected with AKT or Stat3 expression plasmid and their control cells. (**B**) Representative results (*left*) and statistical analyses (*right*) of Matrigel invasion assay, sorting of side-population (SP) cells by flow cytometry and tumorsphere formation assay in the EphA2-SA-expressed NPC cells transfected with AKT or Stat3 expression plasmid and their control cells. (**C**) Representative immunohistochemistry showing the expression levels of p-AKT, p-Stat3, Sox-2, c-Myc and ALDH1A1 in the mice lung metastases of NPC cells expressing EphA2-WT, EphA2-SA and their control cells. Scale bars = 50 μm. Numbers represent mean ± SD. $^{**}P < 0.01$; $^{***}P < 0.001$; $^{****}P < 0.0001$; ns, no significance.

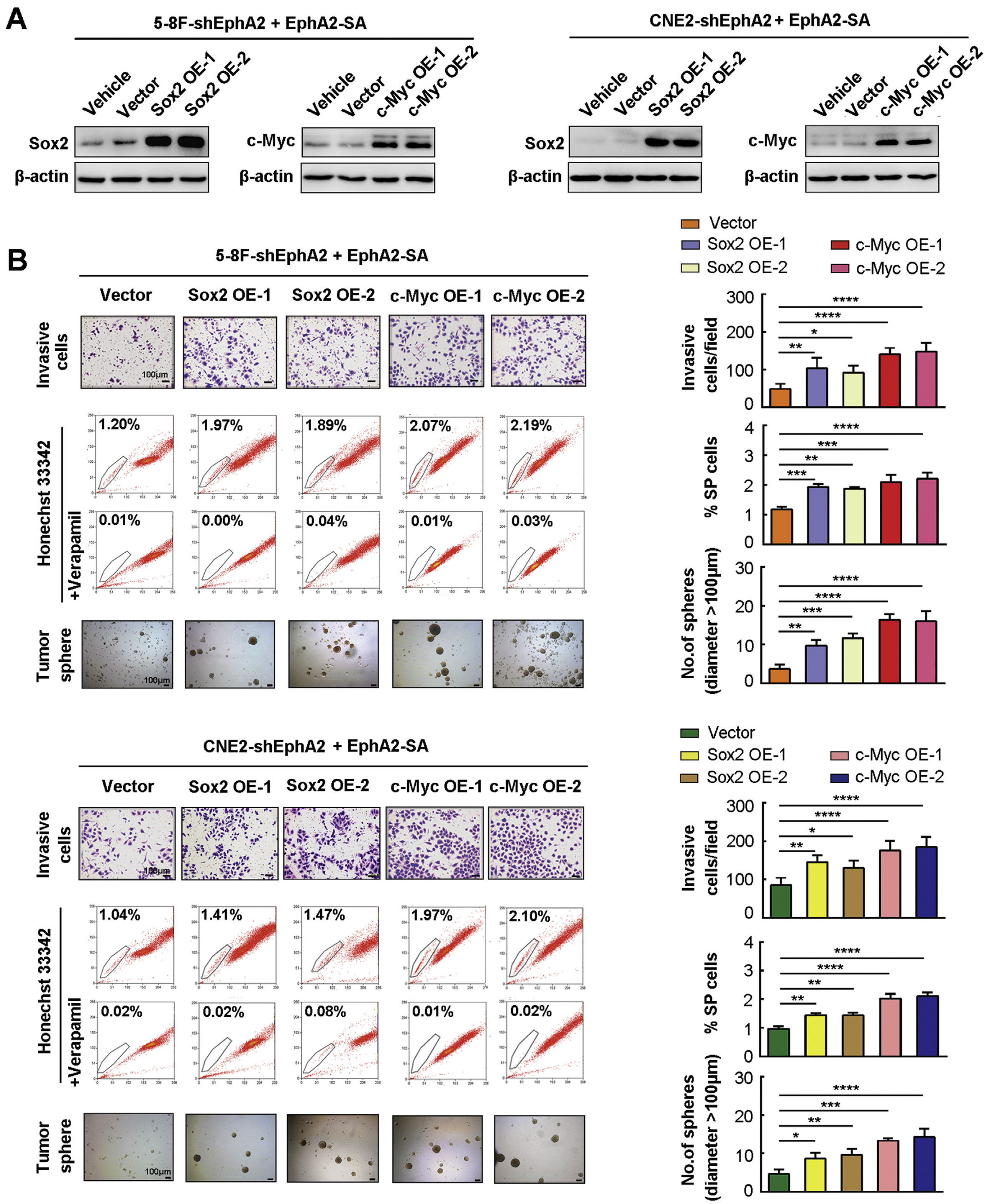

Fig. 7. Sox-2 and c-Myc are the effectors of pS897-EphA2-dependent NPC cell invasion and stem properties. (**A**) Western blot analysis showing the expression levels of Sox-2 and c-Myc in the EphA2-SA-expressed NPC cells transfected with Sox-2 or c-Myc expression plasmid and their control cells. (**B**) Representative results (*left*) and statistical analyses (*right*) of Matrigel invasion assay, sorting of side-population (SP) cells by flow cytometry and tumorsphere formation assay in the EphA2-SA-expressed NPC cells transfected with Sox-2 or c-Myc expression plasmid and their control cells. Numbers represent mean ± SD. *$P < 0.05$; **$P < 0.01$; ***$P < 0.001$; ****$P < 0.0001$.

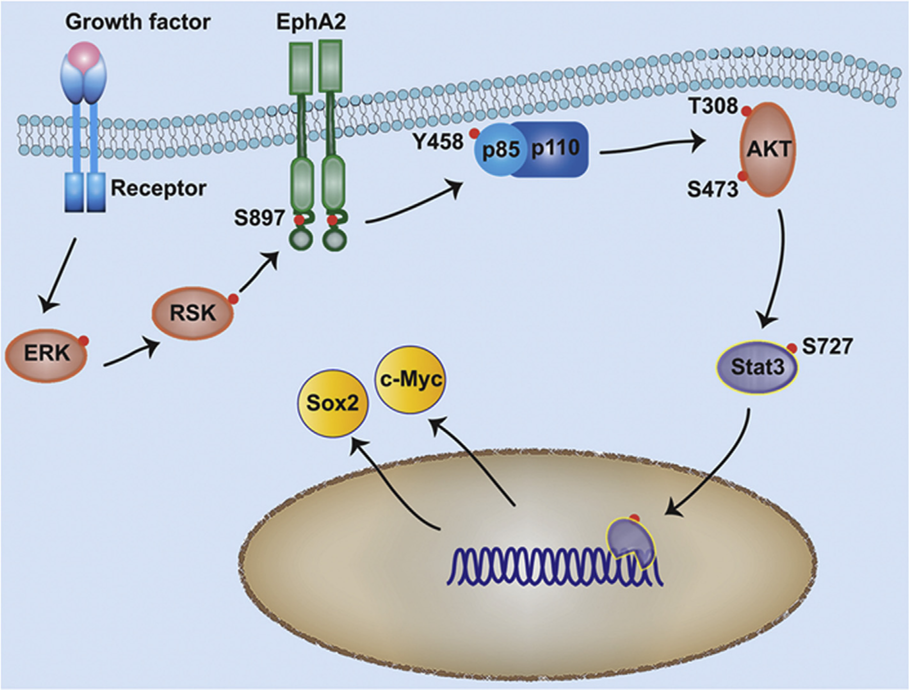

Fig. 8. A model for pS897-EphA2-dependent NPC cell invasion and metastasis and stem properties. EphA2 is phosphorylated at S897 by growth factor receptor/ERK/RSK signaling by a ligand-independent manner, and phosphorylation of EphA2 at S897 activates downstream AKT via PI3K, followed by Stat3 activation and upregulation of Sox-2 and c-Myc that maintain pS897-EphA2-dependent NPC cell invasion and metastasis and stem properties.

Stat3, Sox-2 and c-Myc expressions in the NPCs (Supplemental Fig. 4). Together, these results indicate that pS897-EphA2 appears to be associated with the activation of AKT/Stat3 signaling and upregulation of Sox-2 and c-Myc in the NPCs, which might contribute to clinical tumor progression.

3.9. ERK/RSK controls FBS-induced pS897-EphA2 in NPC cells

It has been reported that AKT and RSK regulate fetal bovine serum (FBS)-induced and ligand-independent pS897-EphA2 in cancer cells [7,13,14], in which AKT or RSK directly phosphorylates EphA2 at S897. Therefore we investigated whether AKT and RSK are also involved in FBS-induced pS897-EphA2 in the NPC cells. 5–8F and CNE2 NPC cells were pre-incubated with PI3K inhibitor (LY294002), AKT inhibitor (MK-2206), MEK inhibitor (U0126) or RSK inhibitor (LJH685) for 30min and then stimulated with FBS for 30min. Western blot analysis showed that FBS induced pS897-EphA2; pretreatment with MEK inhibitor or RSK inhibitor abrogated FBS-induced pS897-EphA2; FBS-induced pS897-EphA2 was not inhibited by LY294002 or MK2206, while AKT phosphorylation was significantly inhibited; FBS and all the inhibitors had no effect on the posphorylation of EphA2 at Y588 (Supplemental Fig. 5). The results indicate that ERK/RSK but not PI3K/AKT signaling pathway controls FBS-induced ligand-independent pS897-EphA2 in NPC cells in a tyrosine kinase activity-independent manner.

4. Discussion

In this study, we found that pS897-EphA2 was upregulated in the high metastatic NPCs, positively correlated with NPC lymphonode and distant metastasis, and was an independent predictor for overall survival, suggesting that pS897-EphA2 plays a crucial role in clinical NPC metastasis. To determine the effects of pS897-EphA2 on the metastasis and stem properties of NPC cells, we established NPC cell lines expressing the equal levels of exogenous EphA2-WT and EphA2-S897A using endogenous EphA2 knockdown cells, an appropriate cell model for comparing the differences of biological functions in the EphA2 and EphA2-S897A. Using the established cell lines, we observed that S897A mutation abolished the effects of EphA2 on NPC cell invasion, metastasis, and stem properties. Our results demonstrate that pS897-EphA2 is indispensable for EphA2-dependent NPC cell invasion, metastasis and stem properties, which is in agreement with previous reports in other cancers [7,11–14].

EphA2 is an emerging drug target in solid tumors. Various therapeutic strategies targeting EphA2, such as monoclonal antibody, kinase inhibitor dasatinib, EphA2 ligand Ephrin-A1, ligand-mimic peptides against EphA2 and RNA interference, have been developed [46]. It has been reported that a new ATP-competitive EphA2 RTK inhibitor, ALW-II-41-27, effectively inhibits EphA2-mediated NSCLC growth [47], intrahepatic cholangiocarcinoma metastasis [48] and melanoma resistance to Vemurafenib [49] *in vitro* and *in vivo*. Our results demonstrate that pS897-EphA2 is indispensable for EphA2-dependent NPC cell invasion, metastasis and stem properties, indicating that targeting pS897-EphA2 has the same efficacy as targeting EphA2, and pS897-EphA2 is a promising target in NPC therapy. Because all the present therapeutic strategies target EphA2 but not pS897-EphA2, development of specific pS897-EphA2 inhibitors may hold promise for treatment of NPC and perhaps other cancers.

The signals downstream of pS897-EphA2 underlying its metastasis promotion and cancer stem properties maintenance are still unclear. We found that pS897-EphA2 activated AKT through PI3K in the NPC cells. It has been reported that EphA2 activates PI3K and downstream AKT by interacting with the p85 regulatory subunit of PI3K [36–40]. Our results not only support previous publications, but also indicate that pS897-EphA2 mediates EphA2-activating PI3K/AKT. We also found that pS897-EphA2 activated Stat3 signaling in the NPC cells, and further showed that it activated Stat3 through AKT, which is in agreement with previous reports [41,42]. Next, we determined whether AKT/Stat3 signaling mediates pS897-EphA2-dependent NPC cell invasion and stem properties, and demonstrate that pS897-EphA2 promotes NPC cell invasion and stem properties by activating AKT/Stat3 signaling pathway. Finally we analyzed the effects of c-Myc and Sox-2, the known direct transcriptional targets of Stat3 [44,45], on pS897-EphA2-dependent NPC cell invasion and stem properties. The results suggest that Sox-2 and c-Myc are the effectors of pS897-EphA2-promoting NPC cell invasion and stem properties. Our immunohistochemistry also suggest that pS897-EphA2 contributes to clinical NPC metastasis possibly through activating AKT/Stat3/Sox-2 and c-Myc signaling pathway.

Determination of the mechanism maintaining cancer stemness is one of the most important challenges in current oncology. Our data strongly suggest that pS897-EphA2/AKT/Stat3/Sox-2 and c-Myc axis has an important function in the maintenance of NPC stem properties, highlighting the therapeutic potential of this signaling axis in targeting NPC stemness. To our knowledge, it is first time reported that AKT/Stat3/Sox-2 and c-Myc signaling mediates pS897-EphA2-dependent cancer stem properties.

The last question is what phosphorylates EphA2 at S897 in NPC cells. Our results indicate that ERK/RSK but not PI3K/AKT signaling pathway controls FBS-induced and ligand-independent pS897-EphA2 in NPC cells, which is consistent with previous report [14]. As there are multiple growth factors in serum, pS897-EphA2 might be a common mediator of growth factor-induced NPC cancer cell metastasis and stem properties, which could have important implications in understanding the molecular basis of malignant progression for NPC and perhaps other cancers.

In summary, we have demonstrated that pS897-EphA2 is indispensable for EphA2-dependent NPC cell invasion, metastasis and stem properties; pS897-EphA2 promotes NPC cell invasion, metastasis and stem properties by AKT/Stat3/Sox-2 and c-Myc signaling axis; ERK/RSK but not PI3K/AKT signaling controls ligand-independent pS897-EphA2 in NPC cells (Fig. 8). Our data suggest that pS897-EphA2 can serve as an attractive therapeutic target in NPC and perhaps in other cancers.

Conflicts of interest

No potential conflicts of interest were disclosed.

Funding

This work was supported by the National Basic Research Program of China (2013CB910502), the Major Program of National Natural Science Foundation of China (81230053), and the National Natural Science Foundation of China (81874132, 81472801, 81672687).

Acknowledgements

We thank Dr. Bingcheng Wang for providing EphA2 and EphA2-S897A expression and control plasmids.

Appendix A. Supplementary data

Supplementary data to this article can be found online at https://doi.org/10.1016/j.canlet.2018.12.011.

References

[1] K.W. Lo, K.F. To, D.P. Huang, Focus on nasopharyngeal carcinoma, Cancer Cell 5 (2004) 423–428.

[2] A.T. Chan, Current treatment of nasopharyngeal carcinoma, Eur. J. Cancer 47 (Suppl 3) (2011) S302–S303.

[3] A.W. Lee, Y.F. Poon, W. Foo, S.C. Law, F.K. Cheung, D.K. Chan, S.Y. Tung, M. Thaw, J.H. Ho, Retrospective analysis of 5037 patients with nasopharyngeal carcinoma treated during 1976-1985: overall survival and patterns of failure, Int. J. Radiat. Oncol. Biol. Phys. 23 (1992) 261–270.

[4] H. Miao, B. Wang, Eph/ephrin signaling in epithelial development and homeostasis, Int. J. Biochem. Cell Biol. 41 (2009) 762–770.

[5] H. Miao, B. Wang, EphA receptor signaling–complexity and emerging themes, Semin. Cell Dev. Biol. 23 (2012) 16–25.

[6] E.B. Pasquale, Eph receptors and ephrins in cancer: bidirectional signalling and beyond, Nat. Rev. Canc. 10 (2010) 165–180.

[7] H. Miao, D.Q. Li, A. Mukherjee, H. Guo, A. Petty, J. Cutter, J.P. Basilion, J. Sedor, J. Wu, D. Danielpour, et al., EphA2 mediates ligand-dependent inhibition and ligand-independent promotion of cell migration and invasion via a reciprocal regulatory loop with Akt, Cancer Cell 16 (2009) 9–20.

[8] J. Huang, D. Xiao, G. Li, J. Ma, P. Chen, W. Yuan, F. Hou, J. Ge, M. Zhong, Y. Tang, et al., EphA2 promotes epithelial-mesenchymal transition through the Wnt/β-catenin pathway in gastric cancer cells, Oncogene 33 (2014) 2737–2747.

[9] E. Binda, A. Visioli, F. Giani, G. Lamorte, M. Copetti, K.L. Pitter, J.T. Huse, L. Cajola, N. Zanetti, F. DiMeco, et al., The EphA2 receptor drives self-renewal and tumorigenicity in stem-like tumor-propagating cells from human glioblastomas, Cancer Cell 22 (2012) 765–780.

[10] W. Song, Y. Ma, J. Wang, D. Brantley-Sieders, J. Chen, JNK signaling mediates EPHA2-dependent tumor cell proliferation, motility, and cancer stem cell-like properties in non-small cell lung cancer, Cancer Res. 74 (2014) 2444–2454.

[11] H. Kawai, M. Kobayashi, N. Hiramoto-Yamaki, K. Harada, M. Negishi, H. Katoh, Ephexin4-mediated promotion of cell migration and anoikis resistance is regulated by serine 897 phosphorylation of EphA2, FEBS Open Bio 3 (2013) 78–82.

[12] K.H. Paraiso, T.M. Das, B. Fang, J.M. Koomen, I.V. Fedorenko, J.K. John, H. Tsao, K.T. Flaherty, V.K. Sondak, J.L. Messina, et al., Ligand-independent EPHA2 signaling drives the adoption of a targeted therapy-mediated metastatic melanoma phenotype, Cancer Discov. 5 (2015) 264–273.

[13] H. Miao, N.W. Gale, H. Guo, J. Qian, A. Petty, J. Kaspar, A.J. Murphy, D.M. Valenzuela, G. Yancopoulos, D. Hambardzumyan, et al., EphA2 promotes infiltrative invasion of glioma stem cells in vivo through cross-talk with Akt and regulates stem cell properties, Oncogene 34 (2015) 558–567.

[14] Y. Zhou, N. Yamada, T. Tanaka, T. Hori, S. Yokoyama, Y. Hayakawa, S. Yano, J. Fukuoka, K. Koizumi, I. Saiki, et al., Crucial roles of RSK in cell motility by catalysing serine phosphorylation of EphA2, Nat. Commun. 6 (2015) 7679.

[15] K. Shanmugaratnam, L.H. Sobin, The World Health Organization histological classification of tumours of the upper respiratory tract and ear. a commentary on the second edition, Cancer 71 (1993) 2689–2697.

[16] N. Hiramoto-Yamaki, S. Takeuchi, S. Ueda, K. Harada, S. Fujimoto, M. Negishi, H. Katoh, Ephexin4 and EphA2 mediate cell migration through a RhoG-dependent mechanism, J. Cell Biol. 190 (2010) 461–477.

[17] X.Y. Yang, C.P. Ren, L. Wang, H. Li, C.J. Jiang, H.B. Zhang, M. Zhao, K.T. Yao, Identification of differentially expressed genes in metastatic and non-metastatic nasopharyngeal carcinoma cells by suppression subtractive hybridization, Cell. Oncol. 27 (2005) 215–223.

[18] Q.Y. He, H.M. Yi, H. Yi, T. Xiao, J.Q. Qu, L. Yuan, J.F. Zhu, J.Y. Li, Y.Y. Wang, L.N. Li, et al., Reduction of RKIP expression promotes nasopharyngeal carcinoma invasion and metastasis by activating Stat3 signaling, Oncotarget 6 (2015) 16422–16436.

[19] X.P. Feng, H. Yi, M.Y. Li, X.H. Li, B. Yi, P.F. Zhang, C. Li, F. Peng, C.E. Tang, J.L. Li, et al., Identification of biomarkers for predicting nasopharyngeal carcinoma response to radiotherapy by proteomics, Cancer Res. 70 (2010) 3450–3462.

[20] B. Zhang, J.Q. Qu, L. Xiao, H. Yi, P.F. Zhang, M.Y. Li, R. Hu, X.X. Wan, Q.Y. He, J.H. Li, et al., Identification of heat shock protein 27 as a radioresistance-related protein in nasopharyngeal carcinoma cells, J. Canc. Res. Clin. Oncol. 138 (2012) 2117–2125.

[21] P.F. Zhang, G.Q. Zeng, R. Hu, C. Li, H. Yi, M.Y. Li, X.H. Li, J.Q. Qu, X.X. Wan, Q.Y. He, et al., Identification of flotillin-1 as a novel biomarker for lymph node metastasis and prognosis of lung adenocarcinoma by quantitative plasma membrane proteome analysis, J. Proteomics 77 (2012) 202–214.

[22] Z. Zhang, M. Li, G. Zhang, P. Fang, H. Yao, Z. Xiao, Z. Chen, Identification of human gastric carcinoma biomarkers by differential protein expression analysis using ^{18}O labeling and nanoLC-MS/MS coupled with laser capture microdissection, Med. Oncol. 27 (2010) 296–303.

[23] M.Y. Li, F. Peng, J.H. Zuo, H. Yi, C.E. Tang, C. Li, P.F. Zhang, Z.C. Chen, Z.Q. Xiao, Enhancing the stability of ^{18}O-labeled peptides through removal of immobilized trypsin by ZipTips, Anal. Biochem. 408 (2011) 37–45.

[24] L.M. Chi, C.W. Lee, K.P. Chang, S.P. Hao, H.M. Lee, Y. Liang, C. Hsueh, C.J. Yu, I.N. Lee, Y.J. Chang, et al., Enhanced interferon signaling pathway in oral cancer revealed by quantitative proteome analysis of microdissected specimens using ^{16}O/^{18}O labeling and integrated two-dimensional LC-ESI-MALDI tandem MS, Mol. Cell. Proteomics 8 (2009) 1453–1474.

[25] D. Zheng, S. Liao, G. Zhu, G. Luo, S. Xiao, J. He, Z. Pei, G. Li, Y. Zhou, CD38 is a putative functional marker for side population cells in human nasopharyngeal carcinoma cell lines, Mol. Carcinog. 55 (2016) 300–311.

[26] T. Kondo, T. Setoguchi, T. Taga, Persistence of a small subpopulation of cancer stem-like cells in the C6 glioma cell line, Proc. Natl. Acad. Sci. U. S. A. 101 (2004) 781–786.

[27] J. Wang, L.P. Guo, L.Z. Chen, Y.X. Zeng, S.H. Lu, Identification of cancer stem cell-like side population cells in human nasopharyngeal carcinoma cell line, Cancer Res. 67 (2007) 3716–3724.

[28] S.K. Singh, I.D. Clarke, M. Terasaki, V.E. Bonn, C. Hawkins, J. Squire, P.B. Dirks, Identification of a cancer stem cell in human brain tumors, Cancer Res. 63 (2003) 5821–5828.

[29] L. Xin, D.A. Lawson, O.N. Witte, The Sca-1 cell surface marker enriches for a prostate-regenerating cell subpopulation that can initiate prostate tumorigenesis, Proc. Natl. Acad. Sci. U. S. A. 102 (2005) 6942–6947.

[30] J. Qin, J. Ji, R. Deng, J. Tang, F. Yang, G.K. Feng, W.D. Chen, X.Q. Wu, X.J. Qian, K. Ding, et al., DC120, a novel AKT inhibitor, preferentially suppresses nasopharyngeal carcinoma cancer stem-like cells by downregulating Sox2, Oncotarget 6 (2015) 6944–6958.

[31] A. Wu, W. Luo, Q. Zhang, Z. Yang, G. Zhang, S. Li, K. Yao, Aldehyde dehydrogenase 1, a functional marker for identifying cancer stem cells in human nasopharyngeal carcinoma, Cancer Lett. 330 (2013) 181–189.

[32] W.J. Wang, S.P. Wu, J.B. Liu, Y.S. Shi, X. Huang, Q.B. Zhang, K.T. Yao, MYC regulation of CHK1 and CHK2 promotes radioresistance in a stem cell-like population of nasopharyngeal carcinoma cells, Cancer Res. 73 (2013) 1219–1231.

[33] C.F. Yang, L.X. Peng, T.J. Huang, G.D. Yang, Q.Q. Chu, Y.Y. Liang, X. Cao, P. Xie, L.S. Zheng, H.B. Huang, et al., Cancer stem-like cell characteristics induced by EB virus-encoded LMP1 contribute to radioresistance in nasopharyngeal carcinoma by suppressing the p53-mediated apoptosis pathway, Cancer Lett. 344 (2014)

260–271.

[34] C. Scheel, R.A. Weinberg, Cancer stem cells and epithelial-mesenchymal transition: concepts and molecular links, Semin. Canc. Biol. 22 (2012) 396–403.

[35] S.A. Mani, W. Guo, M.J. Liao, E.N. Eaton, A. Ayyanan, A.Y. Zhou, M. Brooks, F. Reinhard, C.C. Zhang, M. Shipitsin, et al., The epithelial-mesenchymal transition generates cells with properties of stem cells, Cell 133 (2008) 704–715.

[36] F.W.B. Fang, D.M. Brantley-Sieders, Y. Hwang, A.J. Ham, J. Chen, Identification and functional analysis of phosphorylated tyrosine residues within EphA2 receptor tyrosine kinase, J. Biol. Chem. 283 (2008) 16017–16026.

[37] A. Pandey, D.F. Lazar, A.R. Saltiel, V.M. Dixit, Activation of the Eck receptor protein tyrosine kinase stimulates phosphatidylinositol 3-kinase activity, J. Biol. Chem. 269 (1994) 30154–30157.

[38] D.M. Brantley-Sieders, J. Caughron, D. Hicks, A. Pozzi, J.C. Ruiz, J. Chen, EphA2 receptor tyrosine kinase regulates endothelial cell migration and vascular assembly through phosphoinositide 3-kinase-mediated Rac1 GTPase activation, J. Cell Sci. 117 (2004) 2037–2049.

[39] S. Chakraborty, M.V. Veettil, V. Bottero, B. Chandran, Kaposi's sarcoma-associated herpesvirus interacts with EphrinA2 receptor to amplify signaling essential for productive infection, Proc. Natl. Acad. Sci. U. S. A. 109 (2012) E1163–E1172.

[40] P. Subbarayal, K. Karunakaran, A.C. Winkler, M. Rother, E. Gonzalez, T.F. Meyer, T. Rudel, EphrinA2 receptor (EphA2) is an invasion and intracellular signaling receptor for Chlamydia trachomatis, PLoS Pathog. 11 (2015) e1004846.

[41] P.K. Vogt, J.R. Hart, PI3K and STAT3: a new alliance, Cancer Discov. 1 (2011) 481–486.

[42] K. Yokogami, S. Wakisaka, J. Avruch, S.A. Reeves, Serine phosphorylation and maximal activation of STAT3 during CNTF signaling is mediated by the rapamycin target mTOR, Curr. Biol. 10 (2000) 47–50.

[43] J.J. Schuringa, H. Schepers, E. Vellenga, W. Kruijer, Ser727-dependent transcriptional activation by association of p300 with STAT3 upon IL-6 stimulation, FEBS Lett. 495 (2001) 71–76.

[44] J. Yang, D. Liao, C. Chen, Y. Liu, T.H. Chuang, R. Xiang, D. Markowitz, R.A. Reisfeld, Y. Luo, Tumor-associated macrophages regulate murine breast cancer stem cells through a novel paracrine EGFR/Stat3/Sox-2 signaling pathway, Stem Cell. 31 (2013) 248–258.

[45] D. Zhao, C. Pan, J. Sun, C. Gilbert, K. Drews-Elger, D.J. Azzam, M. Picon-Ruiz, M. Kim, W. Ullmer, D. El-Ashry, et al., VEGF drives cancer-initiating stem cells through VEGFR-2/Stat3 signaling to upregulate Myc and Sox2, Oncogene 34 (2015) 3107–3119.

[46] M. Tandon, S.V. Vemula, S.K. Mittal, Emerging strategies for EphA2 receptor targeting for cancer therapeutics, Expert Opin. Ther. Targets 15 (2011) 31–51.

[47] K.R. Amato, S. Wang, A.K. Hastings, V.M. Youngblood, P.R. Santapuram, H. Chen, J.M. Cates, D.C. Colvin, F. Ye, D.M. Brantley-Sieders, et al., Genetic and pharmacologic inhibition of EPHA2 promotes apoptosis in NSCLC, J. Clin. Invest. 5 (2014) 2037–2049.

[48] Y. Sheng, J. Wei, Y. Zhang, X. Gao, Z. Wang, J. Yang, S. Yan, Y. Zhu, Z. Zhang, D. Xu, et al., Mutated EPHA2 is a target for combating lymphatic metastasis in intrahepatic cholangiocarcinoma, Int. J. Canc. (2018 Nov 9), https://doi.org/10.1002/ijc.31979.

[49] B. Miao, Z. Ji, L. Tan, M. Taylor, J. Zhang, H.G. Choi, D.T. Frederick, R. Kumar, J.A. Wargo, K.T. Flaherty, et al., EPHA2 is a mediator of vemurafenib resistance and a novel therapeutic target in melanoma, Cancer Discov. 5 (2015) 274–287.